ÖAW IWF

SPACE DEBRIS STUDY GROUP

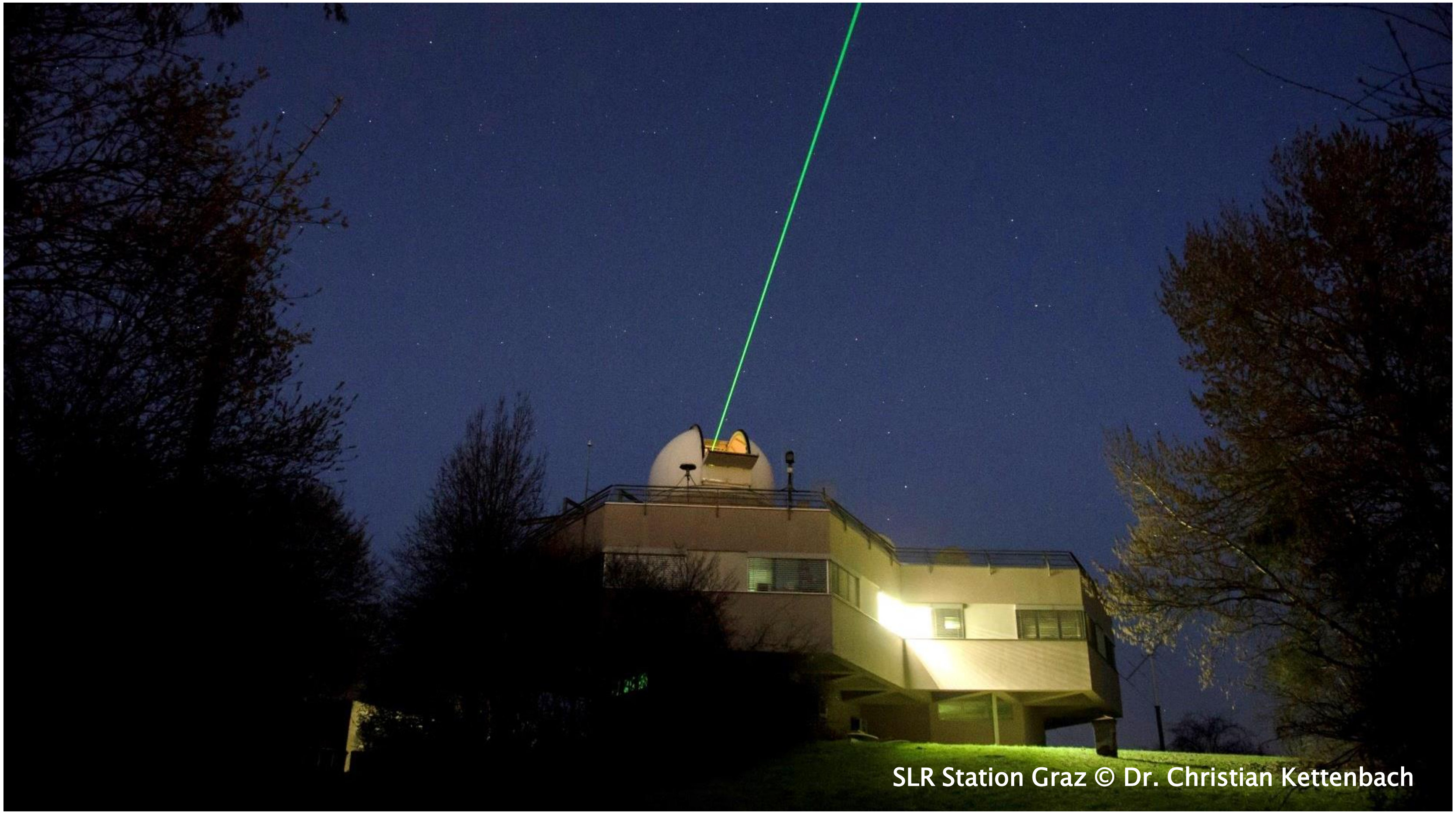

Michael Steindorfer, Georg Kirchner, Franz Koidl, Peiyuan Wang, Sebastian Schneider
1) Space Research Institute, Austrian Academy of Sciences

ÖAW IWF

SDSG OVERVIEW

- Space debris laser ranging activities
  - General space debris laser ranging
  - Improvements / status: (daylight) space debris laser ranging
  - Simultaneous light curves // space debris laser ranging
  - Multistatic campaigns
- Ideas for a campaign within SDSG
- Daniel Kucharski:
  - Updates on tumbling former ILRS satellites
  - Attitude determination methods

GRAZ TRACKING SUMMARY

- Optimum: currently at approx. slant range 2200 km, 10° elevation
- Space debris laser power slightly lower, currently ~12 Watt

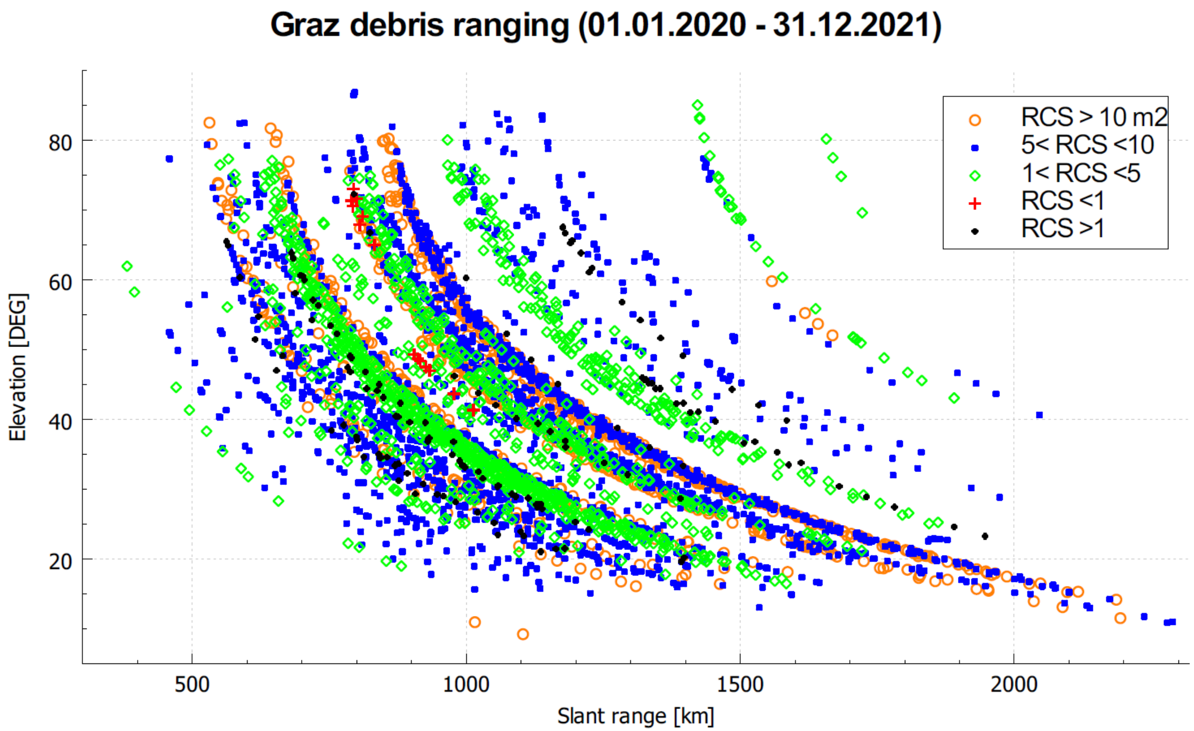

DAYLIGHT DETECTION TOOL

Software development -> Laview -> Python based tool

- Automatic target detection
- Time bias calculation based on orbit
- Multiple targets -> moving (stare & chase) or non moving (tracking)
- „FFP2-mask based testing facility“ --> ZWO ASI camera
- (tiny holes shine some light onto sensor, small dots detected)

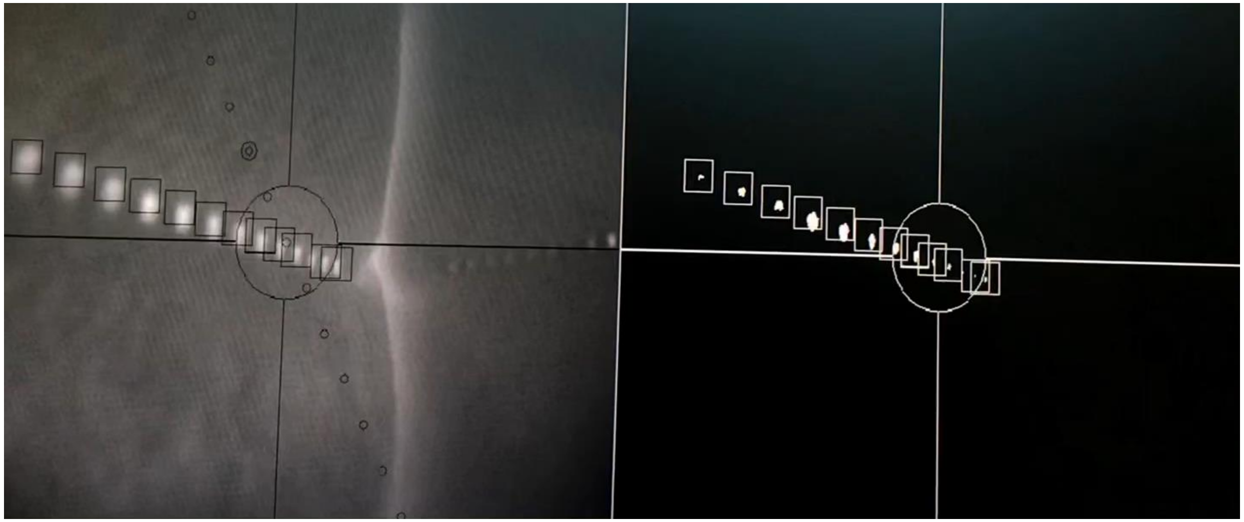

DAYLIGHT SDLR

- Daylight space debris laser ranging:
  - Sessions: 5 test sessions since September (approx. 1 hour each)
  - Types: SL-3, SL-16, CZ-4C, CZ-2C, SL-14, …
  - # optically visible targets during daylight: 35 (also at large sun elevations)
  - Successful daylight passes during last sessions: >10
  - Overall maximum sun elevation: 39°
  - Possible to pre-center targets in field of view
  - Significantly incresing success chances at lower sun elevations

- Outlook: New telescope system for daylight visualization
  - Larger diameter: 25 cm
  - Smaller focal length
  - Smaller sensor at equal field of view
  - Optimized FOV / pixel -> contrast

SDSG / GRAZ UPDATES

- Bistatic measurements -> also allows testing of facilities before active SDLR
  - Recently: Potsdam, Zimmerwald, Stuttgart, Wettzell
  - Planned: Matera, Grasse, ...
  - Graz: „We will do a space debris session in a few hours. Feel free to listen.“
  - Other stations -> contact us if you want to join
  - Good way to test stations receive path
- Light curve measurements / simultaneous to SDLR
  - Large dataset -> used for attitude determination
  - Left: Envisat // Right: H2A-DEB, NORAD 38346

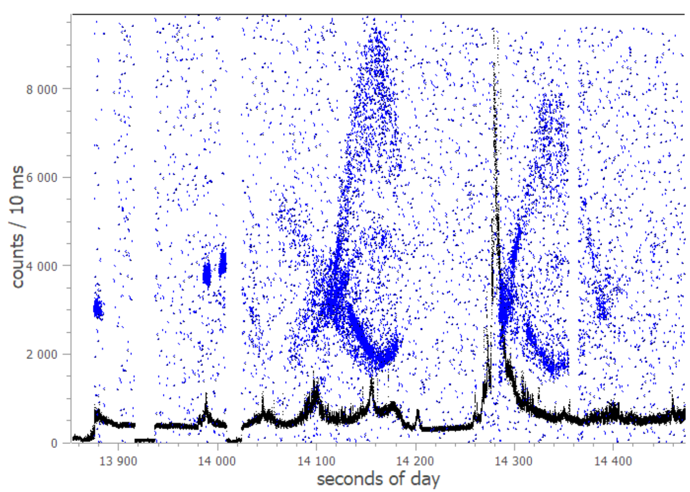

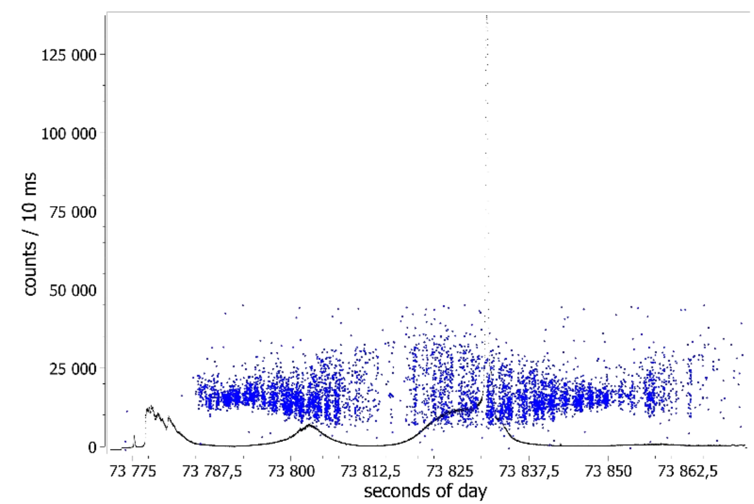

SDSG CAMPAIGN

Space debris laser ranging campaign within SDSG (duration: e.g. 3 months)?

- Selection of 1 target for tracking support
- Potential cooperative targets
  - Low flying rocket bodies with (multiple) retroreflectors
  - E.g. CZ-2C_R/B #28480 (711-914 km), CZ-2C_R/B #31114 (791-878 km)
  - Tumbling high flying satellites
  - Former tumbling ILRS targets Topex, Envisat, Jason
- Predictions or station specific schedules could be sent out by us if needed
- Targets with good orbit could work as multistatic reference targets
- Email to SDSG -> discussion about target selection -> timeframe of campaign

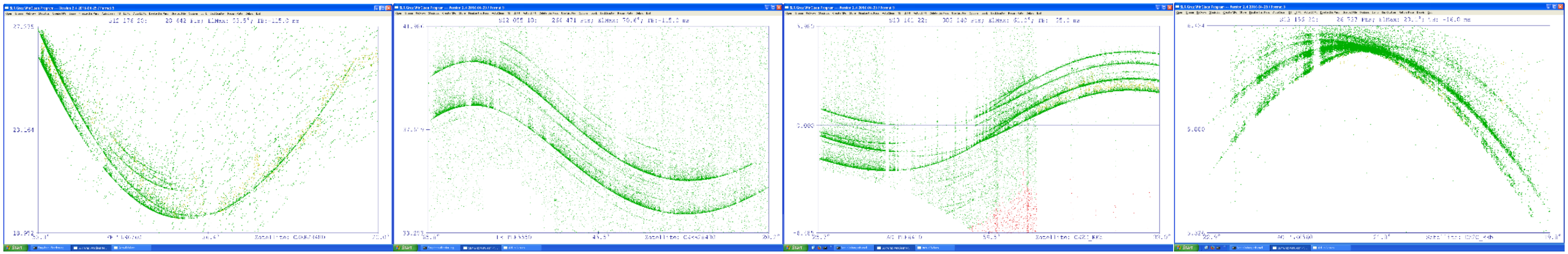

!!! THANK YOU !!!


SLR station Graz
© Christian Kettenbach


Alcantara
© Michael Steindorfer

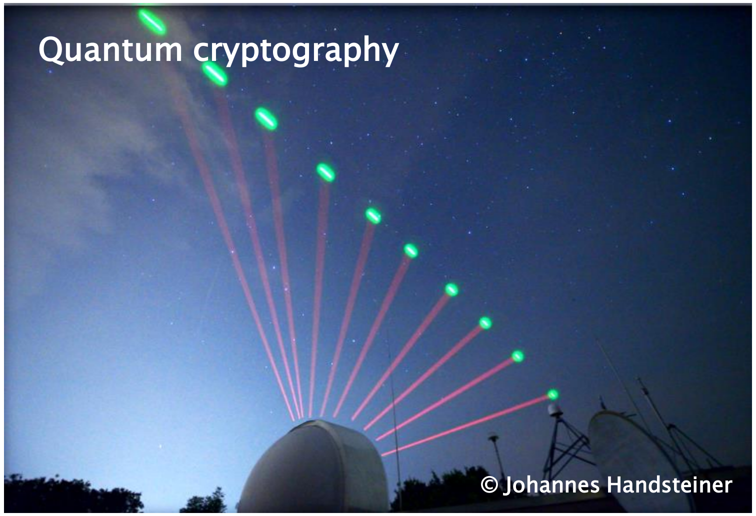
Quantum cryptography
© Johannes Handsteiner

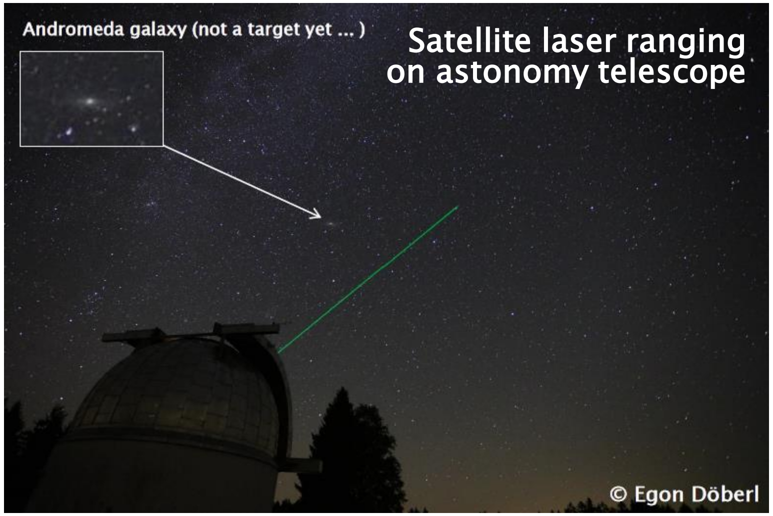
Andromeda galaxy (not a target yet ...)
Satellite laser ranging
on astonomy telescope
© Egon Döberl

Satellite Laser Ranging

- SLR measures range between the ground system and the satellites.
- Routinely operated observational techniques at Graz SLR station are:
    - kHz satellite laser ranging; 2 kHz, 10 ps, 0.4 mJ/pulse
    - space debris laser ranging; 200 Hz, 5 ns, 140 mJ/pulse
    - hypertemporal photometry; kHz-MHz sampling rates

  all at the single-photon sensitivity level realized with the SPAD detectors.
- Graz kHz SLR system operates with a Compensated-SPAD that reacts to the first detected photon – so that the energy of an incoming (retroreflected) pulse is not integrated internally.
- It is beneficial for the space object attitude characterization to operate laser ranging and photometry sub-systems simultaneously and apply data fusion techniques to the collected data for an improved accuracy of the attitude analysis.
- Currently, out of 44 operation SLR stations globally, 11 operate at ≥ 1 kHz repetition rates.

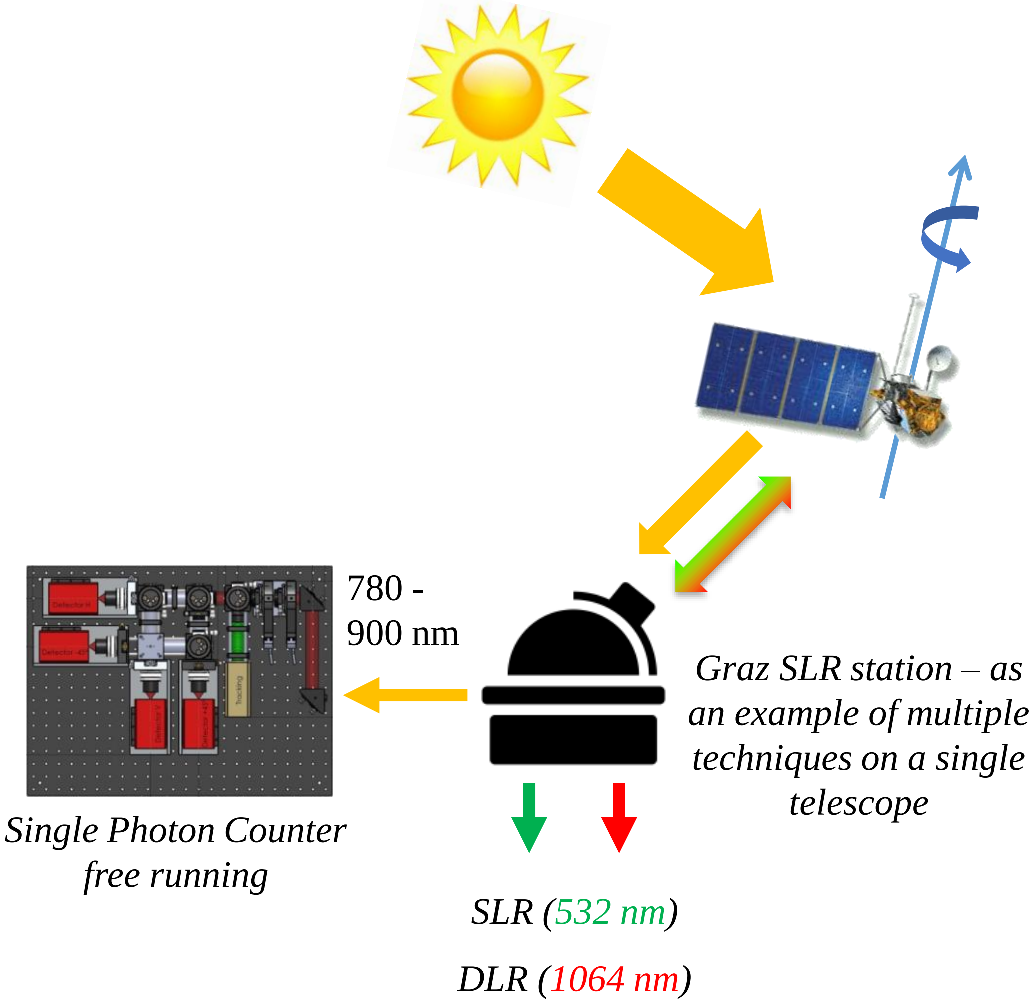

Kirchner G. et al., Light curve measurements with Single Photon Counters at Graz SLR. ILRS Technical Workshop Matera, October 2015.

Satellite attitude tensor and space environment

The satellite inertial attitude depends on the orientation and magnitude of the body spin vector $\boldsymbol{S}$ about which the body spins in a counter-clockwise direction at an angular velocity ω.
The relationship between an external (inertial) reference frame $\mathbb{R}^3$ and the spacecraft body-centered and -fixed coordinate system can be defined by the attitude tensor $\boldsymbol{A}$, which is a product of rotation matrices computed as:

$$\boldsymbol{A} = \boldsymbol{R}_2(-x_P)\boldsymbol{R}_1(-y_P)\boldsymbol{R}_3(\gamma)\boldsymbol{R}_1\left(\frac{\pi}{2} - \delta\right)\boldsymbol{R}_3\left(\frac{\pi}{2} + \alpha\right)$$

$\boldsymbol{R}_1$, $\boldsymbol{R}_2$ and $\boldsymbol{R}_3$: standard rotation matrices about the x, y and z-axis respectively.

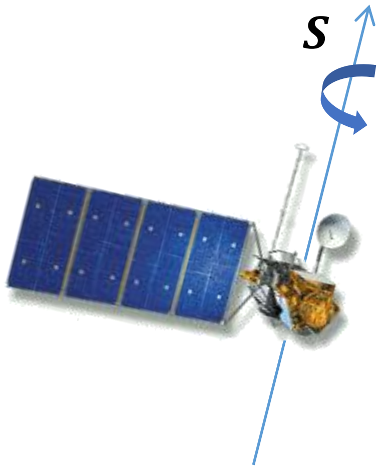

The variables of the transformation depend on the spin vector properties and:
α, δ – correspond to right ascension and declination of $\boldsymbol{S}$ in the case of Earth Centered Inertial reference frame
γ – body rotation angle about $\boldsymbol{S}$, increases at the rate of $\omega = \|\boldsymbol{S}\|$
x_P, y_P – pole coordinates, relative position of $\boldsymbol{S}$ with respect to the satellite body axis.

The parameters of the attitude matrix are not constant and can evolve under the influence of the space environment, such as:

- Earth's gravity field (can be modeled with EGM96, geopotential model)
- Earth's magnetic field (IGRF11/TS05, int. and ext. magnetic field models)
- Solar radiation pressure (TSI and shadow function)
- Earth's reflectivity (albedo) and IR emissivity (CERES)
- Residual atmosphere (JB2008, atm. density model)
- Satellite surface thermal effects (sat. macromodel)
- Electrostatic effects, Van Allen radiation belts (AE-8, AP-8 charged particle models)

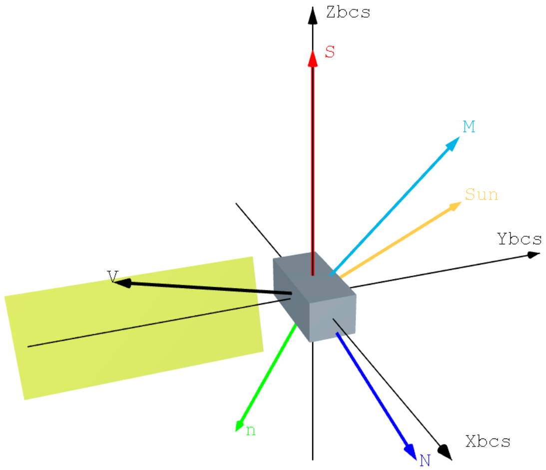

Tumbling example: TOPEX/Poseidon

A)

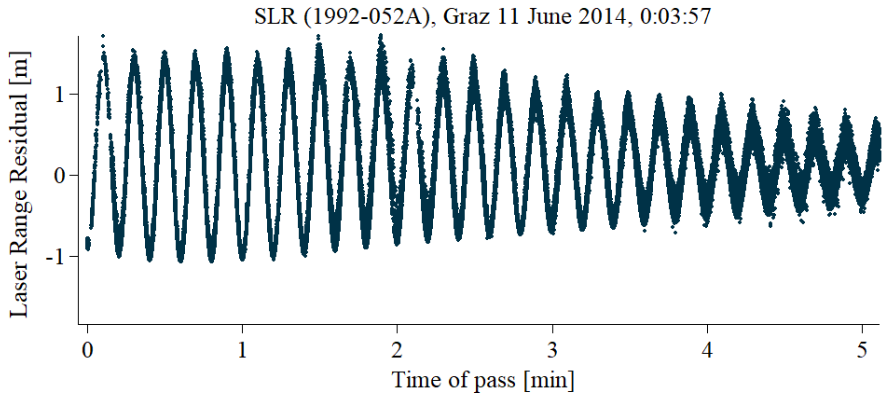

Pass information
Duration: 5m:07s
Data points: 279099
Data rate: 1675.6 Hz

Closest approach
Topo el: 81.9°
Slant range: 1359 km
Phase angle: 69.7°
Sim. app. mag.: 6.2
Solar Beta angle: 16.7°

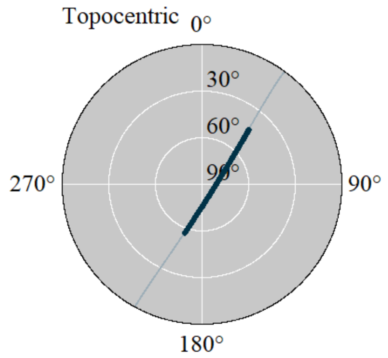

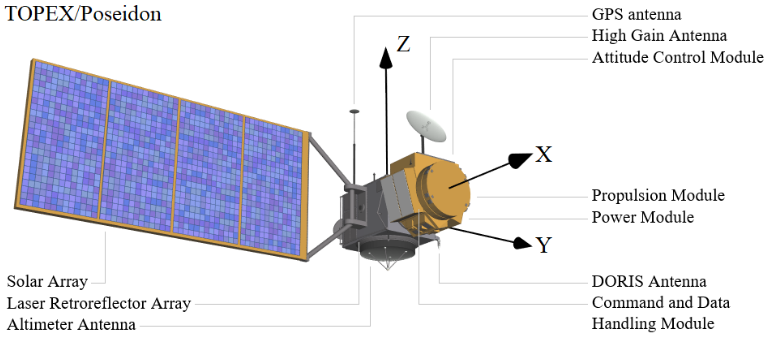

B1)

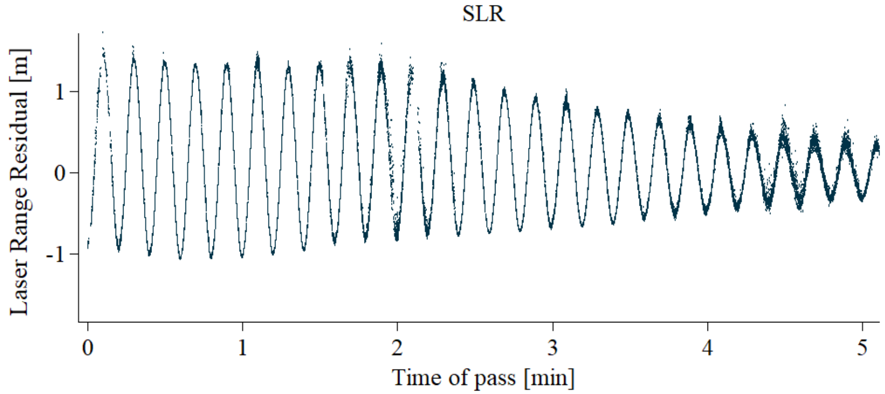

Data averaged

RMS: 0.618 m

C1)

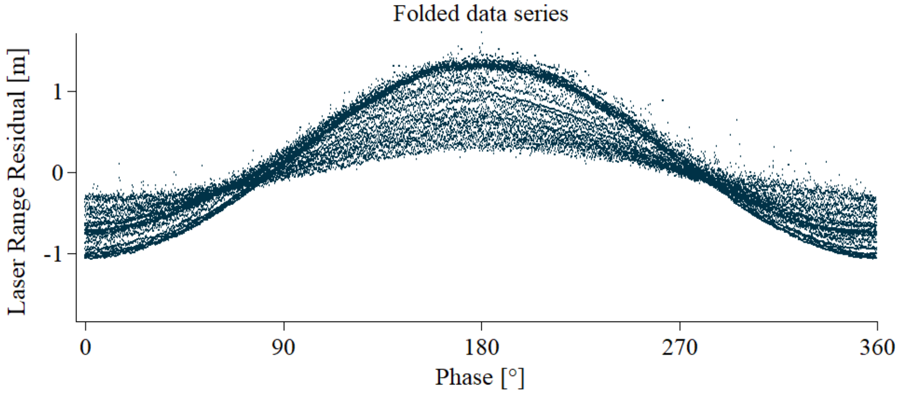

B2)

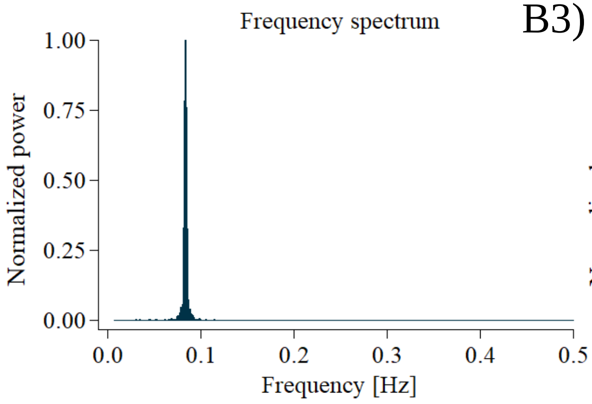

B3)

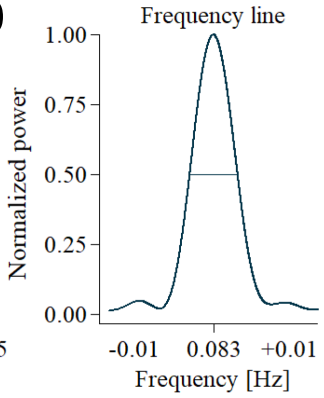

Frequency analysis
Solution profile

Power: 12551.8
Frequency: 0.083 Hz
Period: 11.982 s

FWHM: 3.211 mHz
StdDev: 1.363 mHz
SNR: 61.2
CoVar: 1.634 %

C2)

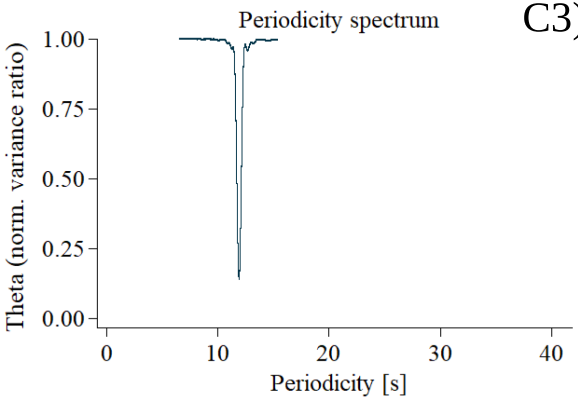

C3)

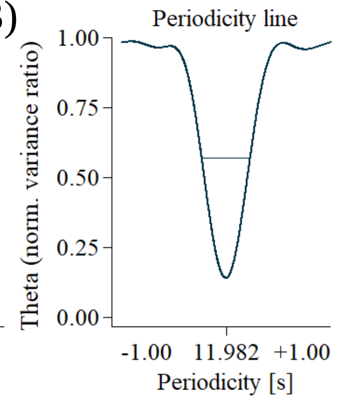

PDM
Solution profile

Theta: 0.141
Period: 11.982 s
Frequency: 0.083 Hz

FWHM: 0.461 s
StdDev: 0.196 s
SNR: 61.2
CoVar: 1.634 %

Tumbling example: Jason-2

A)

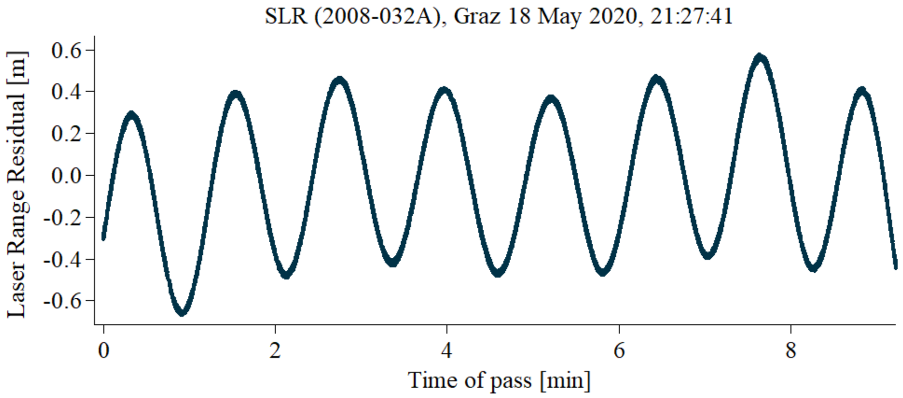

Pass information
Duration: 9m:14s
Data points: 234924
Data rate: 1176.8 Hz

Closest approach
Topo el: 28.2°
Slant range: 2244 km
Phase angle: 84.2°
Sim. app. mag.: 7.7
Solar Beta angle: -6.6°

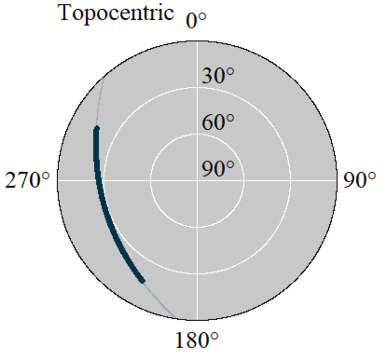

B1)

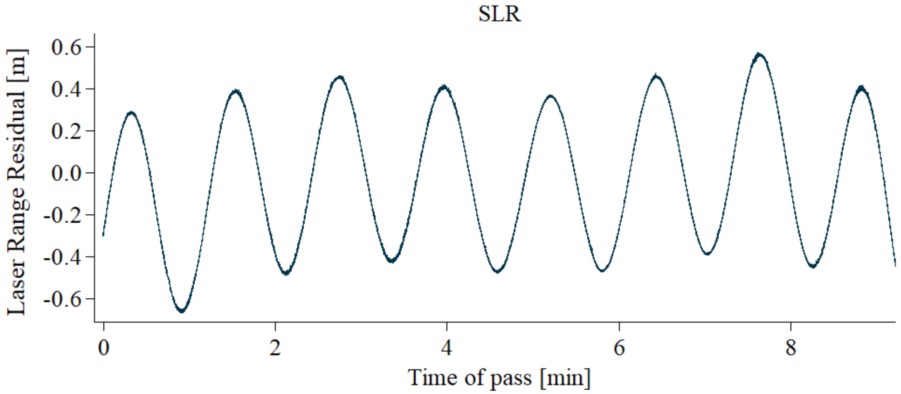

Data averaged

RMS: 0.319 m

C1)

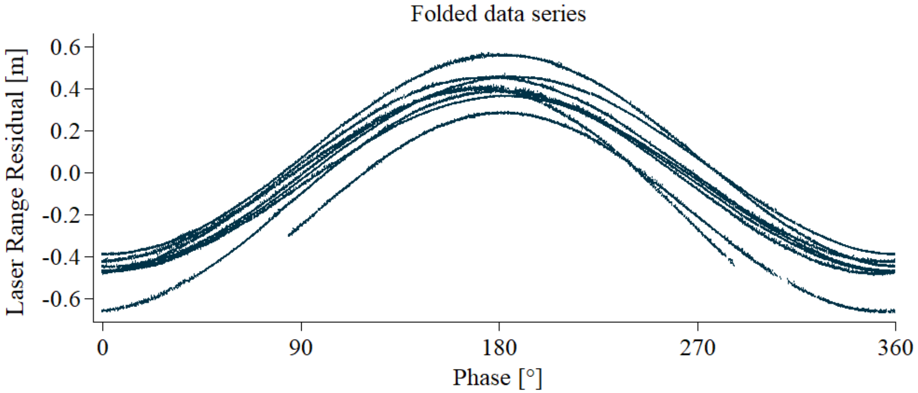

B2)

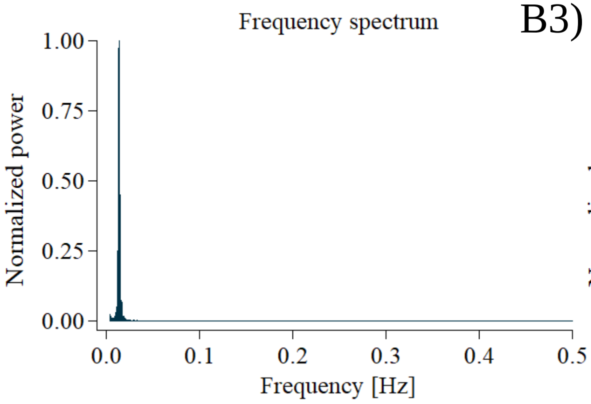

B3)

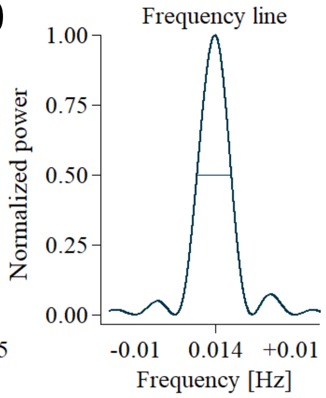

Frequency analysis
Solution profile

Power: 23698.3
Frequency: 0.014 Hz
Period: 73.204 s

FWHM: 1.642 mHz
StdDev: 0.697 mHz
SNR: 19.6
CoVar: 5.106 %

C2)

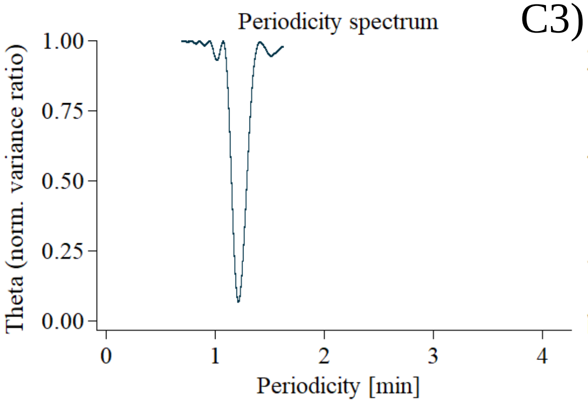

C3)

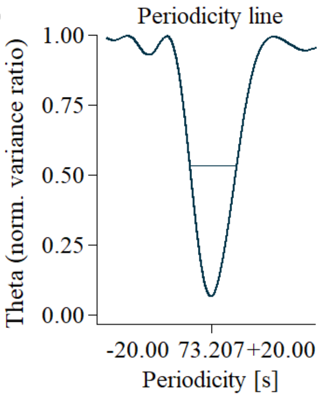

PDM
Solution profile

Theta: 0.066
Period: 73.207 s
Frequency: 0.014 Hz

FWHM: 8.931 s
StdDev: 3.793 s
SNR: 19.3
CoVar: 5.181 %

Tumbling examples

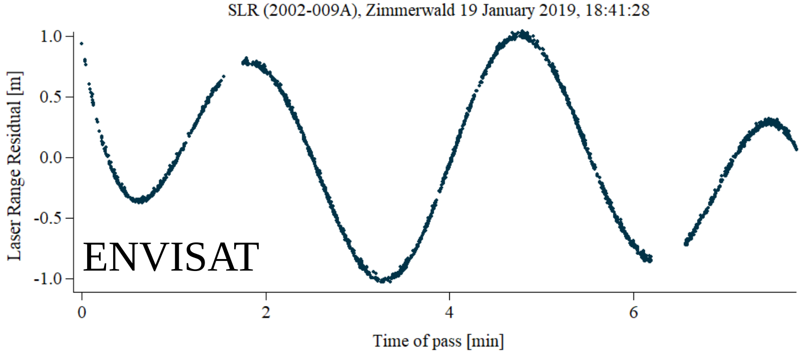

Pass information
Duration: 7m:46s
Data points: 2936
Data rate: 16.6 Hz

Object: ENVISAT
NORAD: 27386
Cospar: 2002-009A
Launch: 1 March, 2002
Apogee alt.: 766 km
Perigee alt.: 764 km
Inclination: 98.2°
Orb. period: 1.7 h
RCS: 18.6 m2

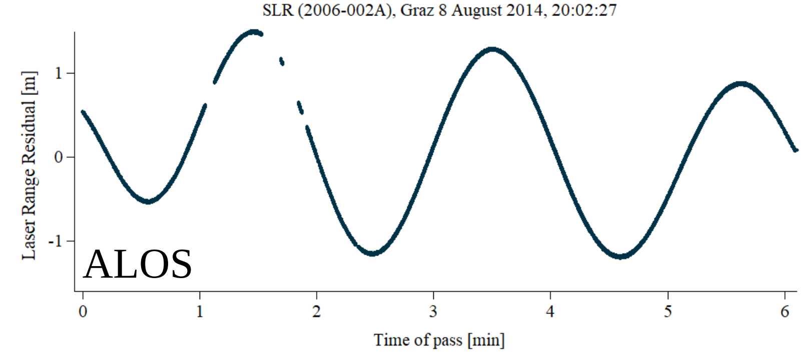

Pass information
Duration: 6m:07s
Data points: 357903
Data rate: 1742.5 Hz

Object: ALOS (DAICHI)
NORAD: 28931
Cospar: 2006-002A
Launch: 24 January, 2006
Apogee alt.: 685 km
Perigee alt.: 682 km
Inclination: 97.9°
Orb. period: 1.6 h
RCS: 13.6 m2

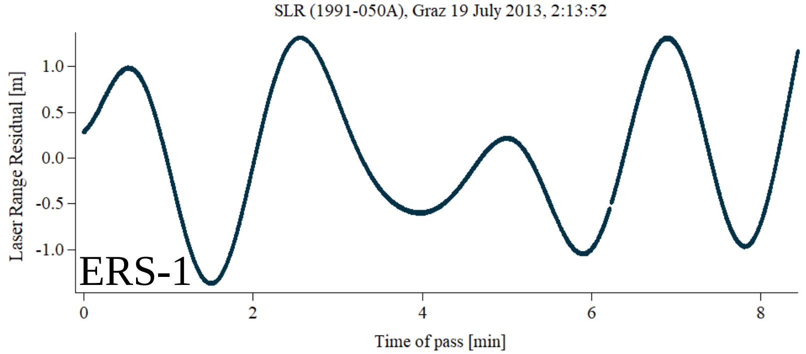

Pass information
Duration: 8m:27s
Data points: 583059
Data rate: 1716.8 Hz

Object: ERS-1
NORAD: 21574
Cospar: 1991-050A
Launch: 17 July, 1991
Apogee alt.: 789 km
Perigee alt.: 742 km
Inclination: 98.7°
Orb. period: 1.7 h
RCS: 10.3 m2

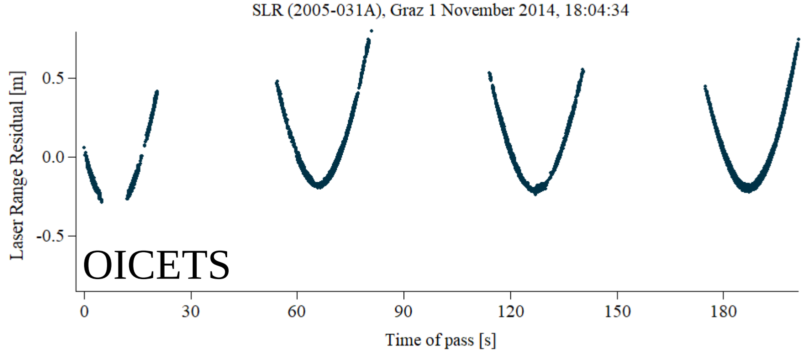

Pass information
Duration: 3m:21s
Data points: 30941
Data rate: 1019.0 Hz

Object: KIRARI (OICETS)
NORAD: 28809
Cospar: 2005-031A
Launch: 23 August, 2005
Apogee alt.: 577 km
Perigee alt.: 551 km
Inclination: 98.1°
Orb. period: 1.6 h
RCS: 1.6 m2

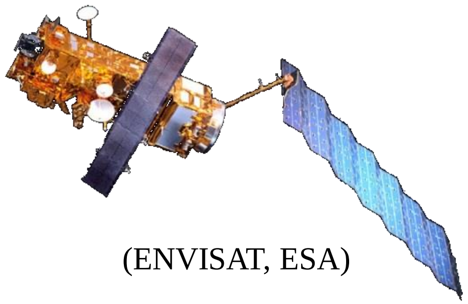

(ENVISAT, ESA)

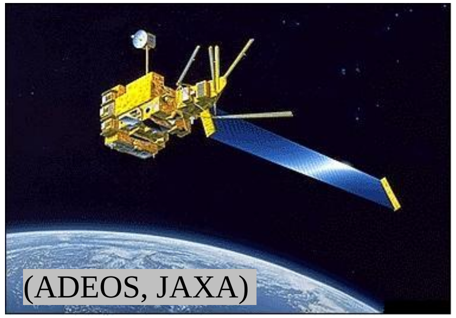

(ADEOS, JAXA)

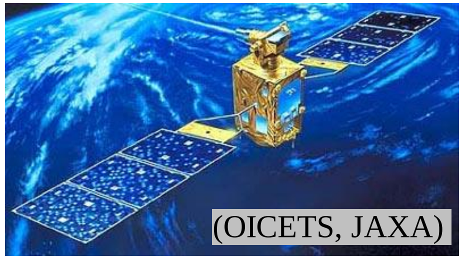

(OICETS, JAXA)

(Jason-1, NASA/CNES)

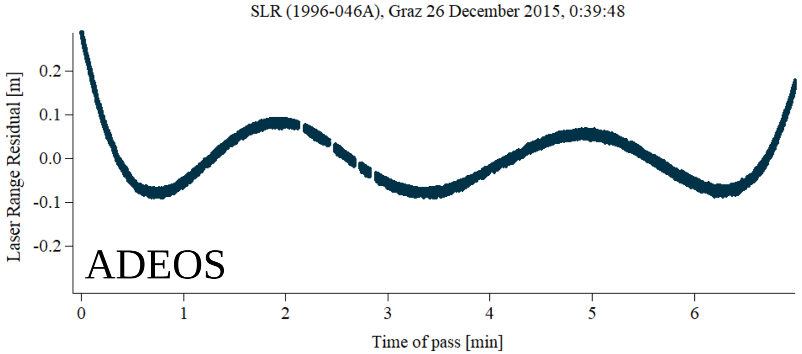

Pass information
Duration: 6m:59s
Data points: 463431
Data rate: 1738.8 Hz

Object: MIDORI (ADEOS)
NORAD: 24277
Cospar: 1996-046A
Launch: 17 August, 1996
Apogee alt.: 795 km
Perigee alt.: 792 km
Inclination: 98.9°
Orb. period: 1.7 h
RCS: 22.2 m2

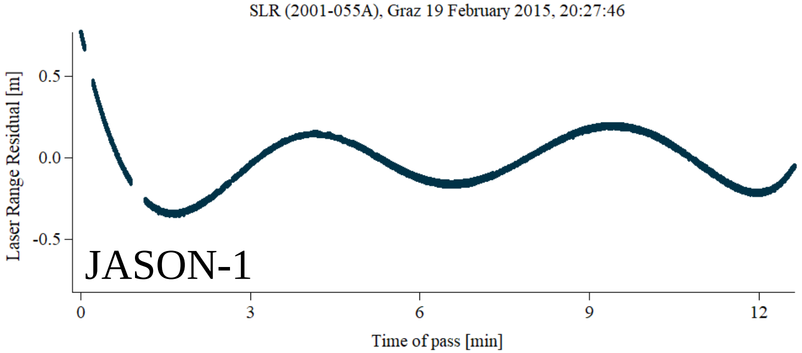

Pass information
Duration: 12m:38s
Data points: 612098
Data rate: 1677.2 Hz

Object: JASON-1
NORAD: 26997
Cospar: 2001-055A
Launch: 7 December, 2001
Apogee alt.: 1332 km
Perigee alt.: 1319 km
Inclination: 66.0°
Orb. period: 1.9 h
RCS: 3.3 m2

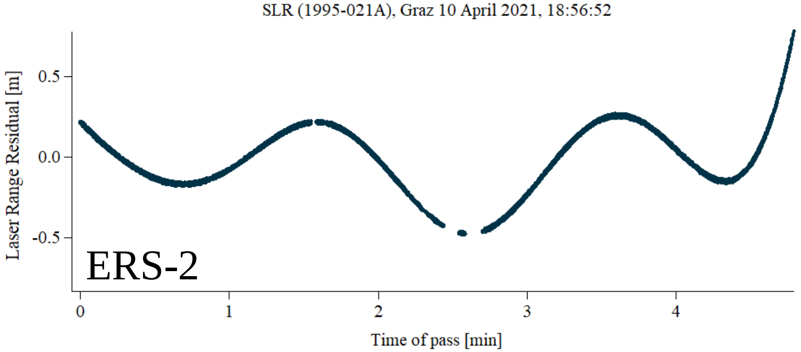

Pass information
Duration: 4m:48s
Data points: 201962
Data rate: 1619.5 Hz

Object: ERS-2
NORAD: 23560
Cospar: 1995-021A
Launch: 21 April, 1995
Apogee alt.: 494 km
Perigee alt.: 489 km
Inclination: 98.5°
Orb. period: 1.6 h
RCS: 9.5 m2

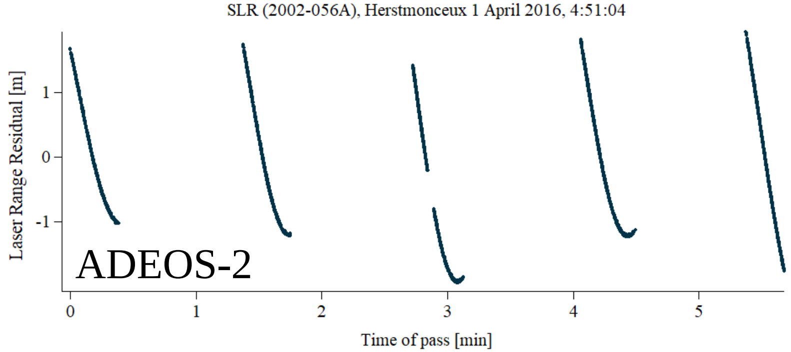

Pass information
Duration: 5m:41s
Data points: 8914
Data rate: 162.7 Hz

Object: MIDORI II (ADEOS-II)
NORAD: 27597
Cospar: 2002-056A
Launch: 14 December, 2002
Apogee alt.: 801 km
Perigee alt.: 799 km
Inclination: 98.6°
Orb. period: 1.7 h
RCS: 17.3 m2

Survey of ILRS Barometers
20-Jan-2022

Van S Husson
vhusson@peraton.com
ILRS NESC

ILRS Barometric Sensors

Barometric Sensor Model	Count	Stations	Total Accuracy (mbar)	Drift per year (mbar)	Temperature Dependence (mbar)
Vaisala PTB220	10	Russian (ROSCOSMOS)	0.15	0.10	0.10
Paroscientific MET4	7	NASA SLR	0.08	0.10	
Paroscientific Digiquartz 740-16B	3	Zimmerwald, Wettzell (7827 and 8834)	0.10	0.10	0.08
Vaisala PTU200	3	Potsdam, Beijing, San Juan	0.15	0.10	0.10
Vaisala PTU300	3	Wuhan, Graz, Grasse	0.15	0.10	0.10
Bosch BMP280	2	Golosiiv, Borowiec	1.00		
Paroscientific Met3A	2	Simeiz, Changchun	0.10	0.10	
Vaisala PTB330	2	Mt Stromlo, Geochang	0.15	0.10	0.10
	2	Apache Point, Komsomolsk-na-Amure			
Davis Instruments Vantage Pro2	1	Kunming	1.00		
Druck DPI 141	1	Herstmonceux	0.15	0.05	0.10
Nippon Electric Instrument RPT-301	1	Tanegashima	0.10	0.10	0.20
Oregon Scientific WMR928N	1	Katzively	1.00		
Ota Keiki Seisakusho Co, LTD OW-7-420	1	Simosato	0.70		
Paroscientific 1016B-01 (appears to be a part number and not a model number)	1	Matera	0.10		
SEAC EMA V (can't find on the internet)	1	San Fernando	0.30		
Vaisala (no model number provided)	1	Shanghai	0.10		
Vaisala BAROCAP	1	Riga	0.15	0.10	0.10
Vaisala WXT520	1	Sejong	0.50		

Legend
Total Accuracy >0.15 millibars
Not provided in Data Sheet

- Barometric sensors have accuracy limitations (i.e. accuracy, stability/drift and temperature dependence)
- A second barometer and yearly calibrations to a known standard hopefully can eliminate drifts in our barometric measurements and kept this bias source at the sub-mm level.

Wrocław University of Environmental and Life Sciences

Identification of range and tropospheric biases from SLR observations to LAGEOS

Mateusz Drożdżewski, Krzysztof Sośnica

Table of content

WROCŁAW UNIVERSITY OF ENVIRONMENTAL AND LIFE SCIENCES

- Simulated barometer bias
- Estimation of tropospheric biases
- Numerical weather models for SLR stations

Observation geometry & correlations

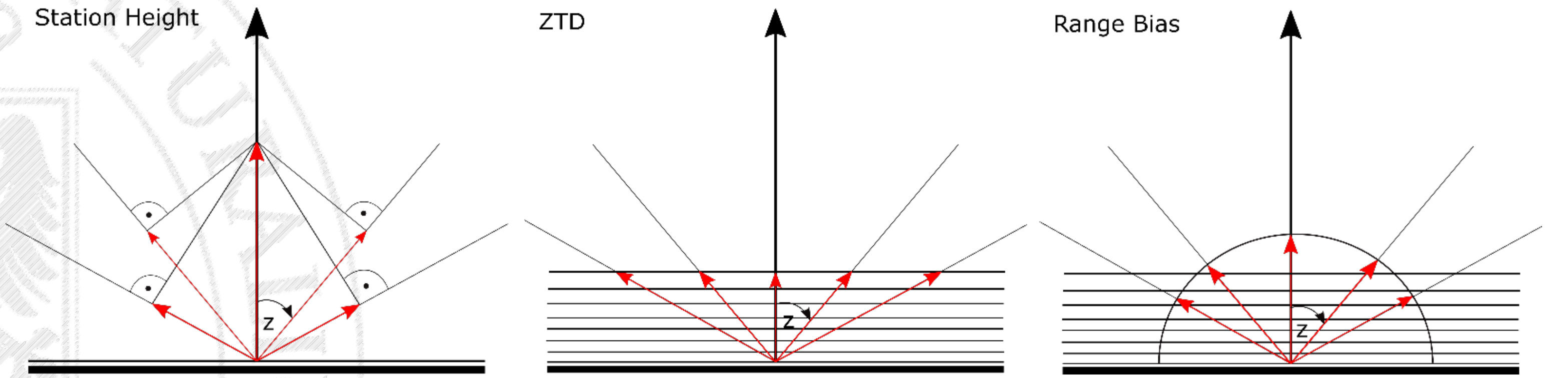

$\delta\rho_h = -\cos(z) * \delta\rho_h(0)$

$\delta\rho_{trp}(z) = mfs(z) * \delta\rho_{trp}(0)$

$\delta\rho_{RB}(z) = \delta\rho_{RB}(0)$

In SLR, zenith tropospheric delay (ZTD), station heights, and range biases are correlated.

The correlation is strongest when only few observations are collected at low elevation angles, e.g., for high-orbiting satellites.

Station heights are one of the most important parameters, because the scale of the reference frame, geocenter motion, and many other parameters rely on the station heights.

A wrong tropospheric delay affects the estimation of station heights because of the correlations.

Artificial pressure bias – a simulation

WROCŁAW UNIVERSITY OF ENVIRONMENTAL AND LIFE SCIENCES

- We apply 5 hPa pressure bias to all SLR stations
- 5 hPa translates into ~11.4 mm differences in tropospheric zenith delay
- We use a priori value of station coordinates from a standard (STD) solution (without a pressure bias)
- We examine following scenarios using real LAGEOS-1/2 observations for 2010-2019:

Estimated parameters / solution	Range bias (RB)	Troposphere zenith delay (TRP)	Station coordinates (CRD)
NEU			x
RB+NEU	x		x
TRP+NEU		x	x
TRP+RGB+NEU	x	x	x

Artificial pressure bias – a simulation

Wrocław University of Environmental and Life Sciences

Graz - 7839

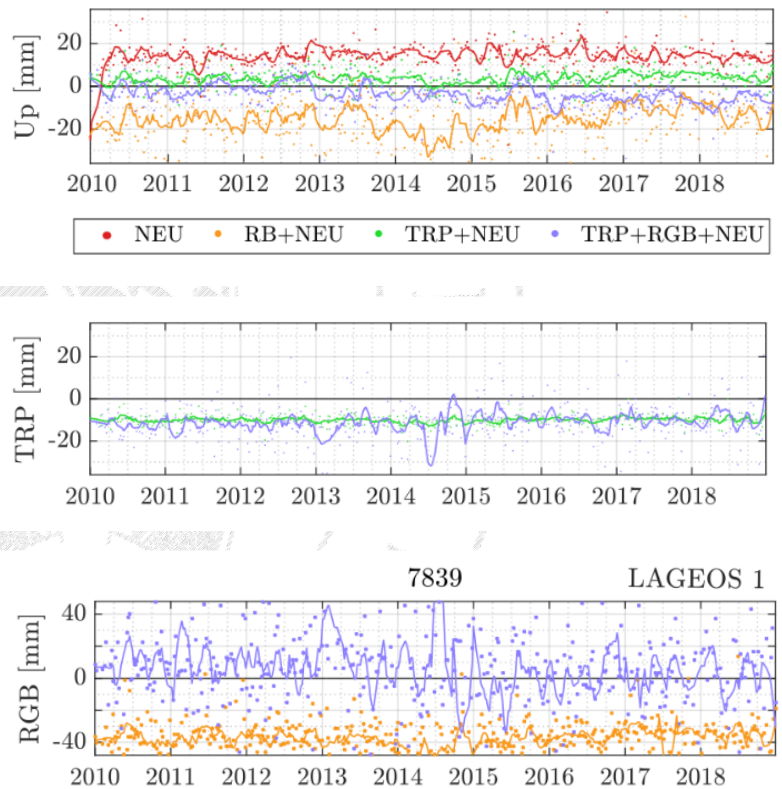

5 hPa (11.4 mm of ZTD) causes a systematic error at the level of +17 mm in station heights (red)

When estimating range biases and coordinates (RB+NEU, orange), the mean bias is **-24 mm.**

Estimation of troposphere delay corrections properly reconstructs ~87% of the pressure bias (remaining error of 1.5 mm).

Solutions with estimated troposphere delay correction are more consistent with a priori coordinates derived from standard solution.

When trying to capture the tropospheric bias by estimating a range bias, the resulting value is -40 mm (orange), but the station height is wrong by +17 mm.

Station heights due to a 5 hPa bias

WROCŁAW UNIVERSITY OF ENVIRONMENTAL AND LIFE SCIENCES

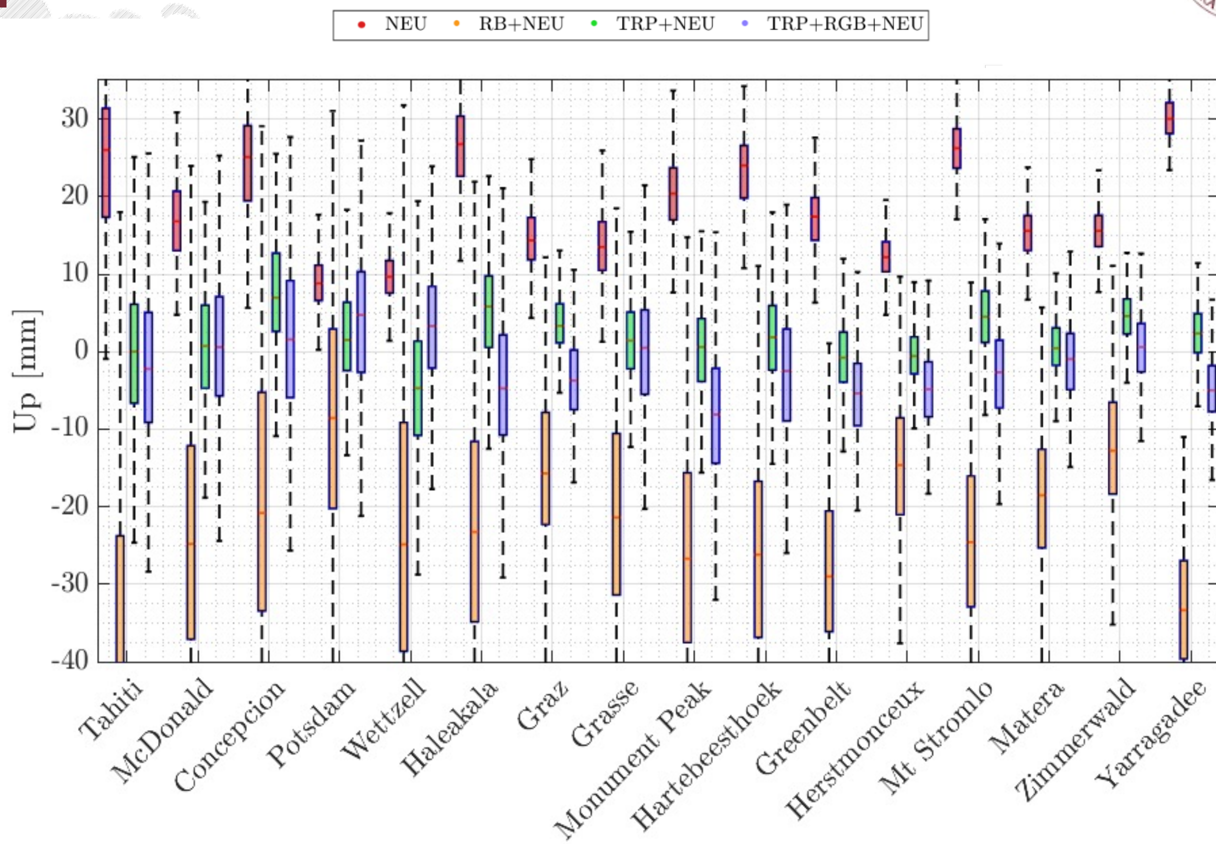

Time series of the Up station component with respect to ITRF2014, for the period 2010 – 2019.

Estimation of range bias to absorb a barometer bias makes everything worse!

NEU ≈ 17 mm

TRP + NEU ≈ 1.5 mm

TRP + RGB + NEU ≈ -2.4 mm

RGB + NEU ≈ -24 mm

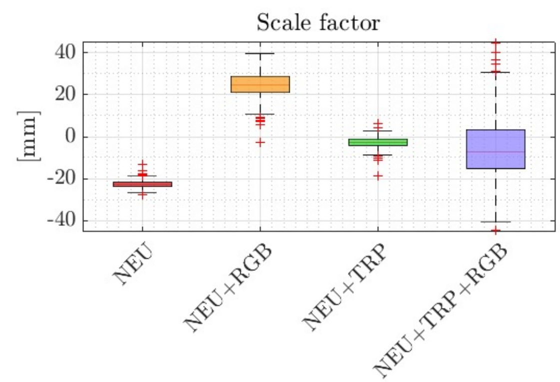

Troposphere correction - reconstruction

WROCŁAW UNIVERSITY OF ENVIRONMENTAL AND LIFE SCIENCES

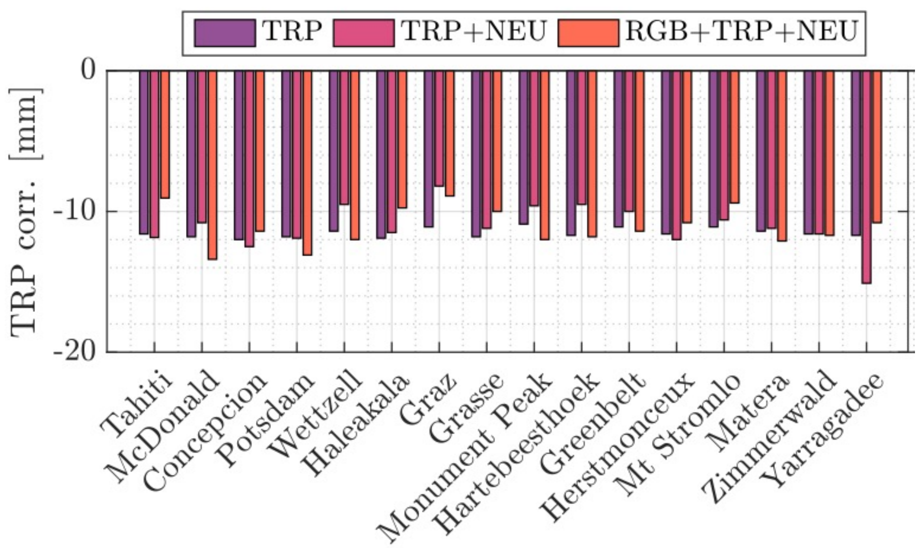

Mean value of estimated troposphere correction ≈12 mm (when estimated) corresponds to artifitial tropospheric bias introduced a priori (11.4 mm).

This means that the estimation of tropospheric biases from SLR data is possible.

However, co-estimation of station coordinates, range biases, and tropospheric biases leads to strong correlations between estimated parameters.

For more results, see:
Drożdżewski, M., Sośnica, K. (2021)
Tropospheric and range biases in Satellite Laser Ranging.
Journal of Geodesy 95, 100. https://doi.org/10.1007/s00190-021-01554-0

Wrocław University of Environmental and Life Sciences

Processing of real LAGEOS data (without artificial biases)

Identification of SLR stations with tropospheric biases - results

SLR stations with tropospheric bias > 1 mm
(greater than 0.44 hPa)
for 2010-2019

But also:

Irkutsk Changchun
Altay Baikonur
Arequipa Graz
Badary Simeiz
Wettzell Zimmerwald
Haleakala Brasilia

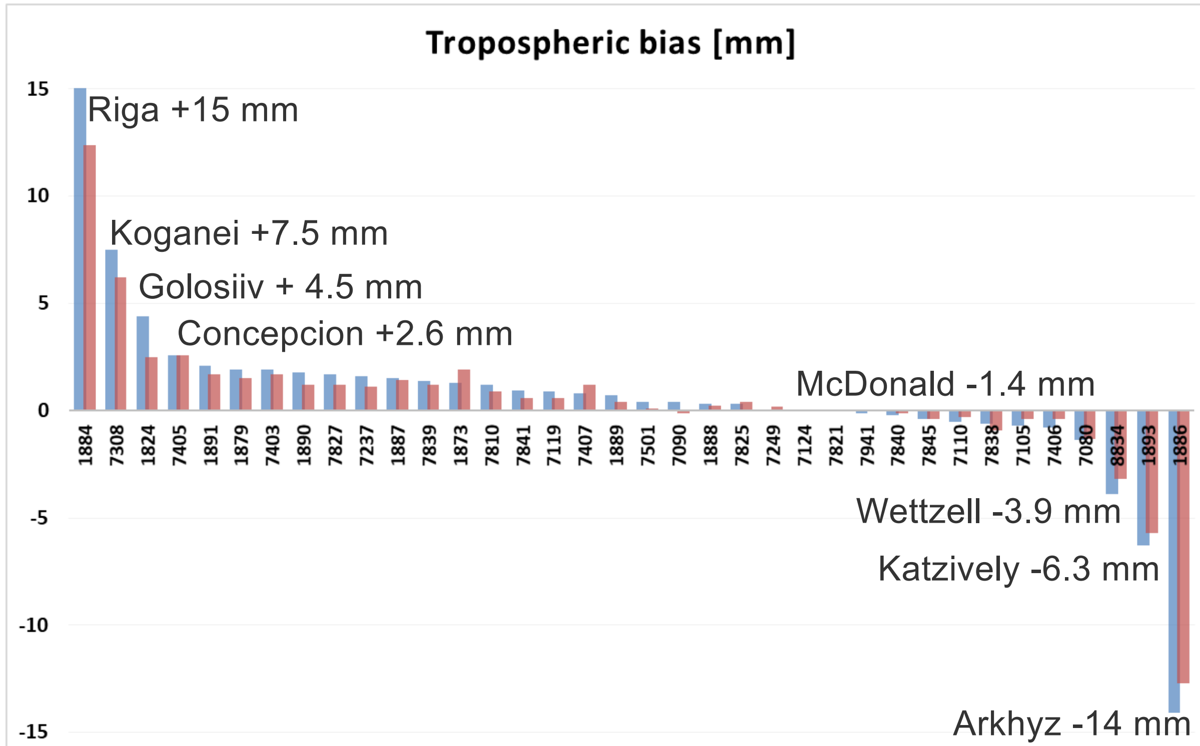

Please note that **tropospheric biases cannot be separated from distance-dependent biases** in the estimation process!

Potential source of tropospheric data for SLR

```
# Vienna Mapping Functions 3 optical (VMF3o) including discrete horizontal gradients calculated from
# ray-tracing data from the VieVS ray-tracer through OPERATIONAL NWM of the ECMWF.
#
# Reference:
# J. Boisits, D. Landskron and J. Boehm, VMF3o: the Vienna Mapping Functions for optical frequencies.
# J Geod (2020). https://doi.org/10.1007/s00190-020-01385-5
#
#
#
# columns:
# -------
# (1) station name
# (2) modified Julian date
# (3) hydrostatic mf coefficient a_h
# (4) wet mf coefficient a_w
# (5) zenith hydrostatic delay (m)
# (6) zenith wet delay (m)
# (7) pressure at the site (hPa)
# (8) temperature at the site (C)
# (9) water vapour pressure at the site (hPa)
# (10) hydrostatic north gradient Gn_h (mm)
# (11) hydrostatic east gradient Ge_h (mm)
# (12) wet north gradient Gn_w (mm)
# (13) wet east gradient Ge_w (mm)
#
1181     59580.00 0.00123089 0.00044140 2.4279 0.0019 1004.72 11.73 12.61 -0.567 -0.509  0.000 -0.001
1824     59580.00 0.00121898 0.00053376 2.3764 0.0020  983.40  4.70  7.66 -0.552 -0.359 -0.001  0.002
1831     59580.00 0.00121995 0.00063002 2.3516 0.0020  973.18  8.43  8.77 -0.511 -0.293  0.003 -0.001
1863     59580.00 0.00115922 0.00032986 1.7610 0.0006  727.54 -4.22  4.15 -0.233  0.174  0.002  0.001
1864     59580.00 0.00115916 0.00033379 1.7605 0.0006  727.34 -4.23  4.15 -0.233  0.173  0.002  0.001
1868     59580.00 0.00117473 0.00054096 2.3924 0.0002  990.39 -20.73  0.64 -0.167 -0.216 -0.001  0.001
1870     59580.00 0.00119806 0.00051963 2.3457 0.0010  970.89 -2.26  4.75 -0.575 -0.107 -0.002  0.001
1873     59580.00 0.00121770 0.00045928 2.3579 0.0014  975.13  5.22  7.77 -0.186 -0.388  0.001 -0.005
1874     59580.00 0.00119804 0.00052107 2.3455 0.0010  970.81 -2.26  4.75 -0.575 -0.107 -0.002  0.001
1879     59580.00 0.00118452 0.00061173 2.3860 0.0002  987.44 -8.68  0.93 -0.416  0.001  0.001 -0.000
1884     59580.00 0.00120372 0.00040681 2.4173 0.0013 1001.70  3.42  6.96 -0.616 -0.371  0.002  0.002
1885     59580.00 0.00120372 0.00040654 2.4174 0.0013 1001.72  3.42  6.96 -0.616 -0.371  0.002  0.002
1886     59580.00 0.00116850 0.00045088 1.9083 0.0006  789.02 -3.54  3.57 -0.285  0.109 -0.001 -0.001
1887     59580.00 0.00121324 0.00057953 2.4275 0.0005 1004.01 -7.84  3.04 -0.149 -0.036 -0.001  0.001
1888     59580.00 0.00119100 0.00042410 2.3875 0.0007  988.93 -2.32  4.55 -0.559 -0.257 -0.003 -0.000
1889     59580.00 0.00119677 0.00049358 2.1822 0.0010  902.51  2.86  4.52 -0.359  0.082 -0.002 -0.001
1890     59580.00 0.00117027 0.00061291 2.4554 0.0002 1015.62 -10.48  0.63 -0.594 -0.275  0.000 -0.000
1891     59580.00 0.00115367 0.00054793 2.3248 0.0002  962.46 -15.11  0.91 -0.536 -0.228  0.000  0.000
1893     59580.00 0.00122512 0.00049250 2.4445 0.0015 1010.95  7.73  8.15 -0.194 -0.383  0.001 -0.006
```

VMF Data Server
Vienna Mapping Functions Open Access Data

https://vmf.geo.tuwien.ac.at/trop_products/SLR/VMF3o/

https://vmf.geo.tuwien.ac.at/

Tropospheric parameters for each day and each SLR station generated on a operational basis with 6h-resolution based on numerical weather models

Latency of the operational products: 24h
(new data at about 18:00 every day for the previous day)

Predictions for the next day generated at 9:00, however, not publically available.

VMF3o pressure records as third independent barometer at SLR stations

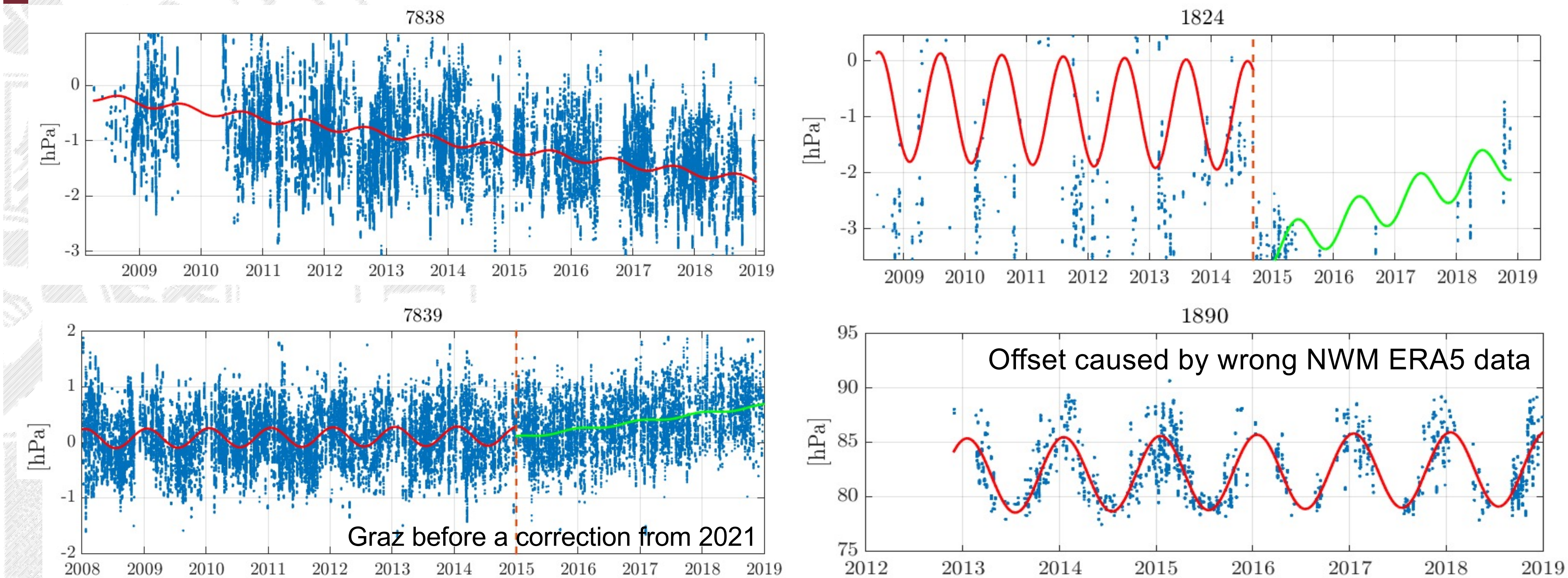

Difference of pressure records derived from in situ measurements and VMF3o
Reference: J. Boisits, D. Landskron and J. Boehm, for VMF3o: the Vienna Mapping Functions for optical frequencies. J Geod (2020). https://doi.org/10.1007/s00190-020-01385-5

VMF3o pressure records as third independent barometer at SLR stations

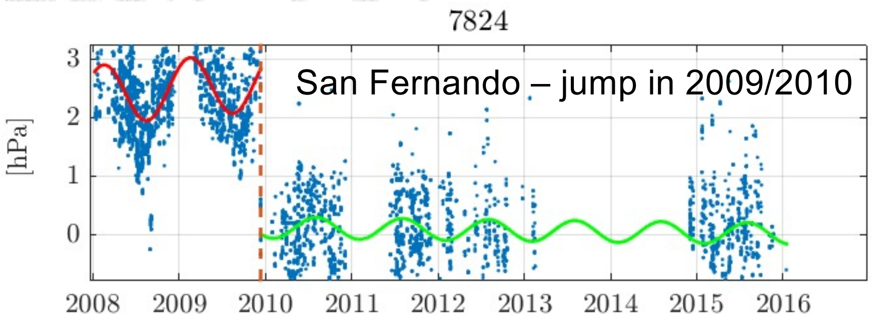

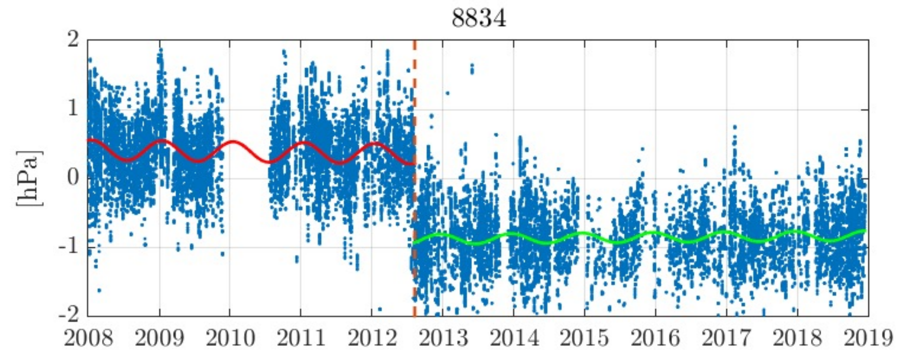

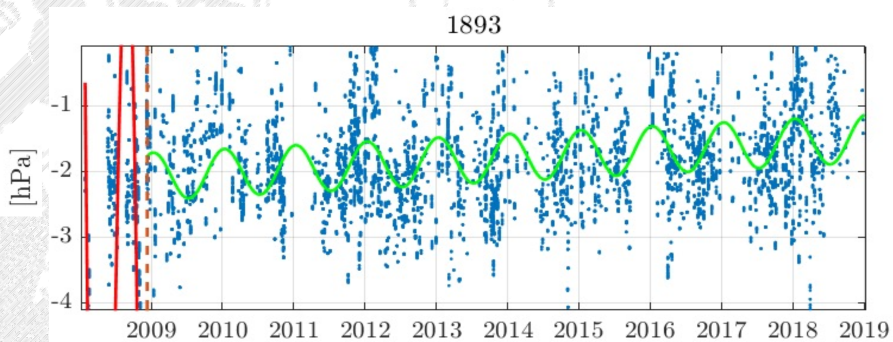

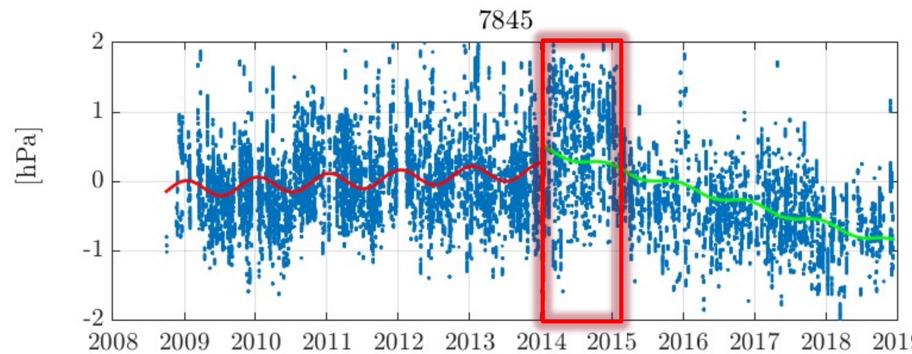

Grasse – 2014-2015 data seem to be wrong?

Comparison between meteo data from SLR normal points and VMF3o

ILRS Website

Borowiec

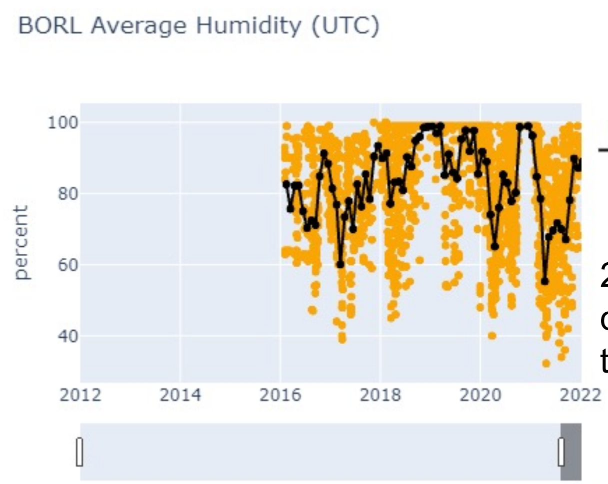

2018/2019
data tightened
to the value of 99%

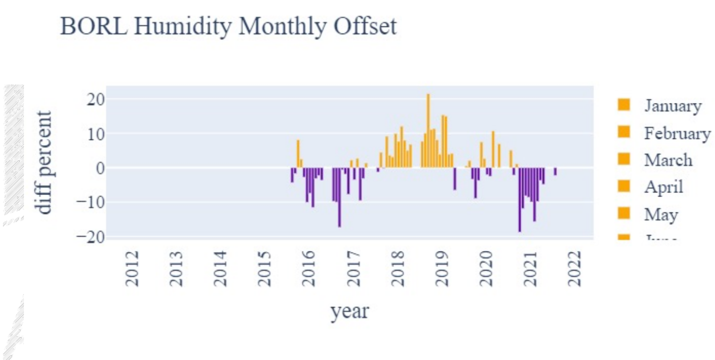

Zimmerwald

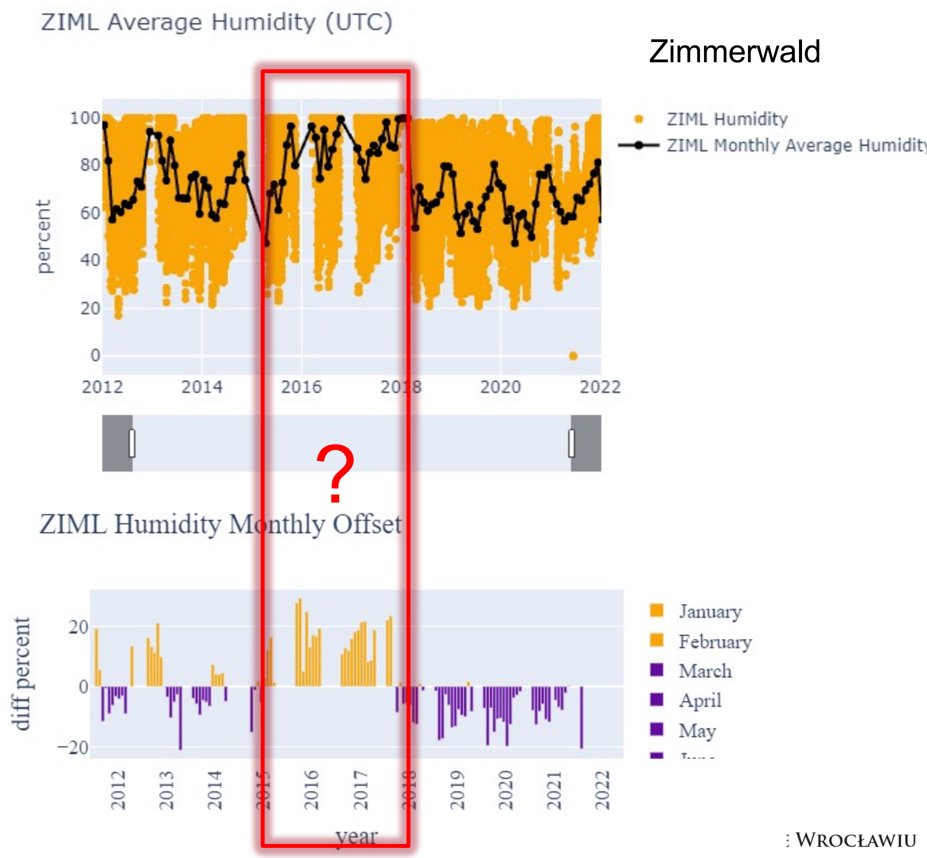

Wrocław University of Environmental and Life Sciences

Thank you for your attention!

Identification of SLR stations with tropospheric biases - results

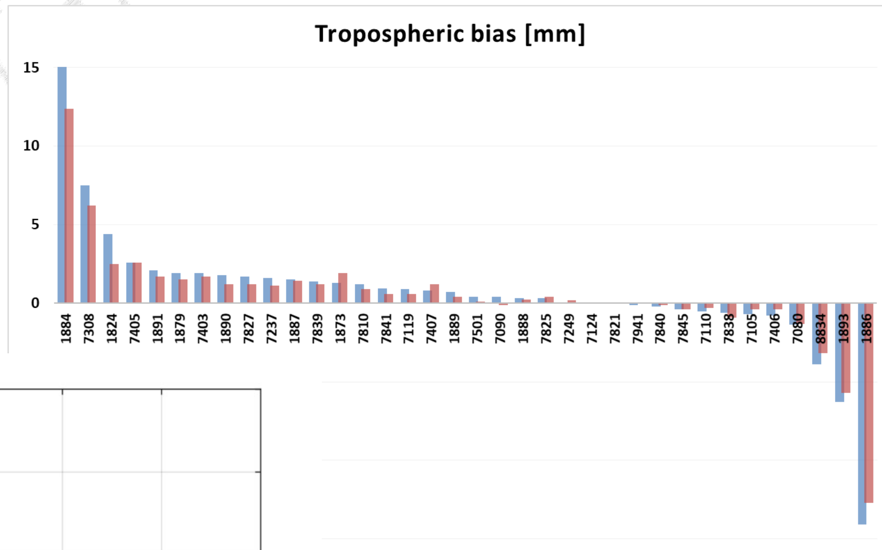

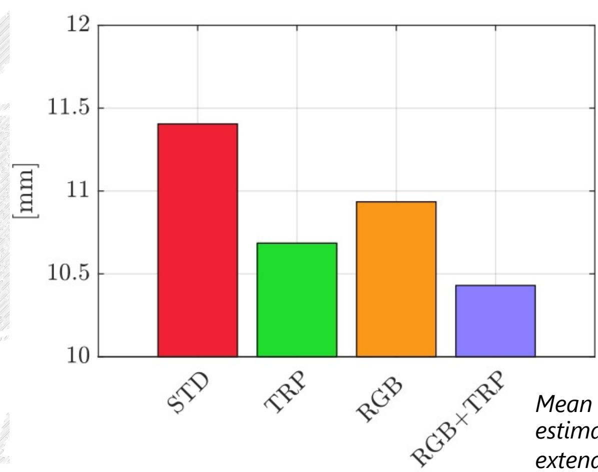

Mean error of the LAGEOS-1/2 solution: estimation of the troposphere reduces the error to a greater extend than estimation of range biases.

Station	TRP [m]	TRP+RB [m]	No obs
1884	0,0154	0,0124	5535
7308	0,0075	0,0062	11768
1824	0,0044	0,0025	4512
7405	0,0026	0,0026	43500
1891	0,0021	0,0017	8799
1879	0,0019	0,0015	15498
7403	0,0019	0,0017	18569
1890	0,0018	0,0012	8228
7827	0,0017	0,0012	7166
7237	0,0016	0,0011	75391
1887	0,0015	0,0015	21518
7839	0,0014	0,0012	71996
1873	0,0013	0,0019	9305
7810	0,0012	0,0009	212380
7841	0,0010	0,0006	52336
7119	0,0009	0,0006	63027
7407	0,0008	0,0012	5251
1889	0,0007	0,0004	9839
7501	0,0004	0,0001	87229
7090	0,0004	-0,0001	324292
1888	0,0003	0,0003	14333
7825	0,0003	0,0004	118951
7249	0,0001	0,0002	12823
7124	0,0000	0,0000	23291
7821	0,0000	0,0000	28282
7941	-0,0001	0,0001	172062
7840	-0,0002	-0,0001	108424
7845	-0,0004	-0,0004	73827
7110	-0,0005	-0,0003	86970
7838	-0,0006	-0,0009	81674
7105	-0,0007	-0,0004	95803
7406	-0,0008	-0,0004	56532
7080	-0,0014	-0,0013	31453
8834	-0,0039	-0,0032	61161
1893	-0,0063	-0,0057	20219
1886	-0,0141	-0,0127	10511